4

Competing Molecular and Radical Pathways in the Dissociation of Halons

4.1 INTRODUCTION

Decomposition chemistry of aliphatic halogenated compounds has been studied in recent years due to its importance in atmospheric chemistry. In the stratosphere, the crucial role played by halogenated molecules in ozone depletion is well known[Navarro *et al.*, 2015; Solomon *et al.*, 2007] and has been widely investigated. Dissociation of halons (halomethanes) may lead to two types of products viz., molecular and radical products and the branching between these has been the subject of many theoretical and experimental studies[Sudbø *et al.*, 1979; Chowdhury, 1991; King and Stephenson, 1978; Krajnovich *et al.*, 1982; Kumaran *et al.*, 1995; Abel *et al.*, 1994]. In the present work, four molecules viz., CF_2Cl_2, CF_2Br_2, $CHBr_3$, and CH_2BrCl were selected for investigation due to their importance in atmospheric chemistry. Molecular halogen elimination, homolytic cleavage of C−X (X=F, Cl, and Br) bond to give radical products, and dehydrohalogenations (HX) are the main dissociation pathways of these molecules. A rich literature on the dissociation chemistry of these molecules exists due to their wide past industrial use and impact on the environment[Zitter *et al.*, 1975; Morrison *et al.*, 1981; Lin and Tsai, 2014; Lyman *et al.*, 1997; Taketani *et al.*, 2005; Talukdar *et al.*, 1992; Yang *et al.*, 2010; Pal *et al.*, 2013; McGivern *et al.*, 2000; Zou *et al.*, 2004; Le Guen *et al.*, 2005; Valero and Truhlar, 2012; Rozgonyi and González, 2008b; Tzeng *et al.*, 1994; Rozgonyi and González, 2008a; Zhou *et al.*, 2006; Lee *et al.*, 2000; McGivern *et al.*, 1999; Chicharro *et al.*, 2017; Zou *et al.*, 2000; Rozgonyi and González, 2002; Hua *et al.*, 2008; Lewerenz *et al.*, 1985; Hsu *et al.*, 2005; Xu *et al.*, 2002; Petro *et al.*, 2004; George *et al.*, 2010; Cameron and Bacskay, 2000; Kalume *et al.*, 2010].

A variety of experimental techniques such as reflected shock wave experiments,[Kumaran *et al.*, 1995] infrared multi-photon dissociation,[Morrison *et al.*, 1981] cavity ring-down absorption spectroscopy,[Lin and Tsai, 2014] ultraviolet laser induced fluorescence,[Taketani *et al.*, 2005] matrix isolation infrared spectroscopy,[George *et al.*, 2010] and detailed quantum chemistry calculations[Cameron and Bacskay, 2000; Kalume *et al.*, 2010] have been used to investigate the dissociation chemistry of these molecules. Photolytic decomposition of CF_2Cl_2 and CF_2Br_2 is one of the primary sources of Cl and Br atoms produced in the atmosphere. Majority of experimental work reported in the literature are focused on the radical product formation and the molecular channels have not been addressed in required detail. Lin et al., have reported a comprehensive account of molecular halogen elimination from halomethanes investigated using cavity ring-down spectroscopy[Lin and Tsai, 2014]. Production mechanisms of molecular products Cl_2 (from CF_2Cl_2) and Br_2 (CF_2Br_2 and $CHBr_3$) have always remained controversial. These processes have been considered to occur via concerted pathways involving a multi-center transition state (TS) in the gas phase[Cameron and Bacskay, 2000]. However, no electronic structure studies characterizing such multi-center TSs have been reported. Alternate proposed pathway for the molecular product formation involves *iso-halons* containing a halogen-halogen bond[Reid, 2014; Huang *et al.*, 2004; Preston *et al.*, 2013; Borin *et al.*, 2016; George *et al.*, 2011; Mereshchenko *et al.*, 2015] and subsequent dissociation. These iso-halons have been identified as reactive intermediates in the condensed phase chemistry of halomethanes[George *et al.*, 2010]. Electronic structure theory has provided insights into the structure and energetics of iso-halons but their role in the gas phase chemistry of halons is not well established[Reid, 2014]. Kalume et al.,[Kalume *et al.*, 2010] have reported

detailed electronic structure calculations (at the CCSD(T)//MP2/aug-cc-pVTZ level of theory) characterizing the radical and molecular dissociation pathways of CF_2Cl_2, CF_2Br_2, and $CHBr_3$. In their calculations, they identified nearly iso-energetic pathways for radical formation and isomerization for all three species. However, they did not locate any multi-center TS for the concerted elimination of Cl_2 or Br_2. For the CH_2BrCl molecule, two radical pathways exist viz., Cl and Br eliminations and the competition between the two pathways have been investigated[Tzeng *et al.*, 1994; Rozgonyi and González, 2008a; Zhou *et al.*, 2006]. Among these two, Br is much more efficient in depleting the stratospheric ozone[Rowland, 1991]. The CH_2BrCl molecule has been utilized, among other halomethanes, as a prototype to study mode selective chemistry due to its ability to decompose via multiple pathways[Shu *et al.*, 2012].

In the present work, the gas phase chemistry of CF_2Cl_2, CF_2Br_2, $CHBr_3$, and CH_2BrCl were investigated. The objective of the present work is to characterize the dissociation dynamics of these important molecules at the atomic level to establish reaction mechanisms. One of the focus points is to study the role of iso-halons in the chemistry of these molecules in the gas phase.

4.2 POTENTIAL ENERGY SURFACE

Electronic structure theory calculations at different level of theories were used to characterize the potential energy surfaces of all the four molecules. Geometries of all the four molecules are shown below.

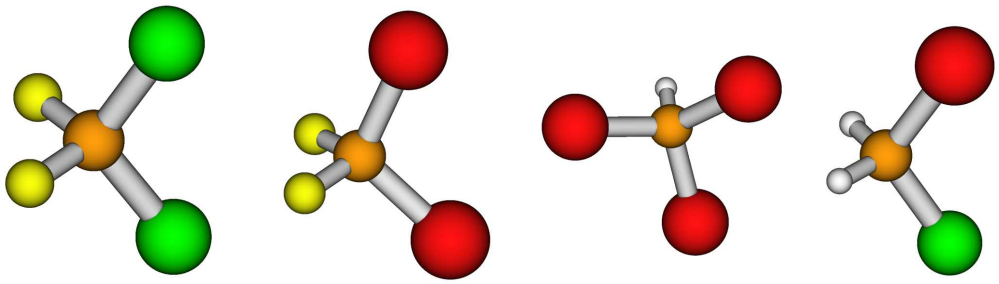

CF_2Cl_2 CF_2Br_2 $CHBr_3$ CH_2BrCl

Energies of all the stationary points are summarized below for all four molecules along with previously reported values. The energies are in kcal/mol and zero point energy not corrected unless specified.

Table 4.1 : Stationary point energies of CF_2Cl_2 dissociation profile computed using different levels of theory. The energies are in kcal/mol and relative to the reactant molecule.

Theory	$Cl + CF_2Cl$	Iso-TS[a]	$F_2C-Cl-Cl$	$CF_2 + Cl_2$	TS1[b]	Ref.
PBE0/6-31G*	78.95	79.44	69.93	84.00	126.56	pw[c]
M06/6-31G*	81.98	86.17	79.38	81.56	132.06	pw
B3LYP/6-31G*	74.53	74.44	64.31	75.67	116.01	pw
B3LYP/6-311G	61.33	73.49	62.35	66.99	99.71	pw
B3LYP/aug-cc-pVDZ	73.78	72.83	62.89	72.11	115.59	pw
MP2/aug-cc-pVTZ	90.23	84.51	87.16	85.81	–	pw
PBE0/6-31G*(ECP)	71.20	82.09	71.92	85.35	113.41	pw
CCSD(T)/aug-cc-pVTZ//MP2/aug-cc-pVTZ[d]	78.9	80.0	69.25	71.3	–	[Kalume *et al.*, 2010]

[a] connects reactant with the $F_2C-Cl-Cl$ isomer
[b] concerted TS connecting reactant with the $CF_2 + Cl_2$ products
[c] present work
[d] zero point energy corrected

Table 4.2 : Stationary point energies of CF_2Br_2 dissociation profile computed using different levels of theory. The energies are in kcal/mol and relative to the reactant molecule.

Theory	$Br + CF_2Br$	Iso-TS[a]	$F_2C-Br-Br$	$CF_2 + Br_2$	TS1[b]	Ref.
PBE0/6-31G*	65.29	68.56	49.74	59.99	97.73	pw[c]
M06/6-31G*	63.46	73.65	52.49	58.54	102.45	pw
B3LYP/6-31G*	61.38	64.24	44.49	53.03	102.45	pw
B3LYP/6-311G	55.52	68.34	48.67	54.54	102.45	pw
B3LYP/aug-cc-pVDZ	60.46	63.90	–	51.98	90.09	pw
MP2/aug-cc-pVTZ	80.46	85.86	72.81	69.10	102.89	pw
PBE0/6-31G*(ECP)	53.40	70.17	48.21	54.77	62.94	pw
CCSD(T)/aug-cc-pVTZ//MP2/aug-cc-pVTZ[d]	69.4	73.1	55.9	58.9	87.7	[Kalume *et al.*, 2010]

[a] connects reactant with the $F_2C-Br-Br$ isomer
[b] concerted TS connecting reactant with the $CF_2 + Br_2$ products
[c] present work
[d] zero point energy corrected

Table 4.3 : Stationary point energies of $CHBr_3$ dissociation profile computed using different levels of theory. The energies are in kcal/mol and relative to the reactant molecule.

Theory	$Br + CHBr_2$	Iso-TS[a]	BrHC−Br−Br	$CHBr + Br_2$	$CBr_2 + HBr$	Ref.
PBE0/6-31G*	60.50	60.42	47.65	93.25	69.5	pw[b]
M06/6-31G*	59.22	65.42	54.99	93.12	70.7	pw
B3LYP/6-31G*	53.79	58.45	43.47	84.47	62.7	pw
B3LYP/6-311G	–	55.04	46.96	90.96	68.06	pw
B3LYP/aug-cc-pVDZ	56.92	–	–	82.14	56.85	pw
MP2/aug-cc-pVTZ	78.87	–	68.38	108.42	80.07	pw
PBE0/6-31G*(ECP)	53.52	53.52	53.69	94.43	77.06	pw
CCSD(T)/aug-cc-pVTZ//MP2/aug-cc-PVTZ[c]	65.89	61.35	49.89	89.89	65.9	[Kalume *et al.*, 2010]
B3LYP/aug-cc-pVTZ	–	53.13	41.73	–	–	[Pal *et al.*, 2013]
CAM-B3LYP/aug-cc-pVTZ	–	61.78	51.07	–	–	[Pal *et al.*, 2013]
M06-2X/aug-cc-pVTZ	–	63.33	52.34	–	–	[Pal *et al.*, 2013]
MP2/aug-cc-pVTZ	–	67.73	49.09	–	–	[Pal *et al.*, 2013]
B3LYP/6-311G**	53.1	46.8	41.1	78.1	–	[Huang *et al.*, 2004]
MP4/MP2/LANL2DZ	–	56.8	43.3	–	–	[Petro *et al.*, 2004]

[a] connects reactant with the BrHC−Br−Br isomer
[b] present work
[c] zero point energy corrected

Table 4.4 : Stationary point energies of CH_2BrCl dissociation profile computed using different levels of theory. The energies are in kcal/mol and relative to the reactant molecule.

stationary point	PBE0/6-31G*	MP2/aug-cc-pVTZ	MP2/6-31G*	CCSD(T)// MP2/aug-cc-pVTZ
CH_2BrCl	0.0	0.0	0.0	0.0
$Cl + CH_2Br$	80.46	90.26	79.81	83.4
$Br + CH_2Cl$	68.94	81.07	68.72	74.8
Iso-TS1[(a)]	71.46	79.64	67.5	70.9
$CH_2-Cl-Br$	62.32	74.93	66.48	61.9
CHCl+HBr	94.58	94.61	96.24	86.8
TS3[(b)]	109.91	105.39	120.97	102.88
Isomer-TS2[(c)]	76.97	79.16	85.26	73.4
$CH_2-Br-Cl$	63.18	77.07	76.20	60.3
CHBr+HCl	94.94	93.89	97.06	86.0
TS4[(d)]	116.53	109.47	126.67	107.5
Ref.	pw[(e)]	pw	pw	pw

[(a)] connects reactant with the $H_2C-Cl-Br$ isomer
[(b)] connects reactant with the $CHCl + HBr$ products
[(c)] connects reactant with the $H_2C-Br-Cl$ isomer
[(d)] connects reactant with the $CHBr + HCl$ products
[(e)] present work

Density functional PBE0 level of theory with 6-31G* basis set was selected for direct dynamics simulations. This theory and basis set were selected for two reasons. First, the potential energy profile of halons computed using the selected theory and the benchmark CCSD(T) theory were similar. The CCSD(T)//MP2/aug-cc-pVTZ calculations for dissociation of CF_2Cl_2, CF_2Br_2 and $CHBr_3$ molecules have been reported earlier[Kalume *et al.*, 2010]. For CH_2BrCl, single point energy calculations were performed at the CCSD(T) level of theory using optimized geometries at the MP2/aug-cc-pVTZ level. Energies of all the stationary points at these CCSD(T) calculations along with PBE0/6-31G* level are reported in Table 4.5. The average deviations between PBE0/6-31G* and CCSD(T) calculations over the stationary points are 3.3, 5.4, 3.5, and 5.0 kcal/mol for CF_2Cl_2, CF_2Br_2, $CHBr_3$, and CH_2BrCl, respectively. The second reason for choosing the PBE0/6-31G* level of theory is the low computational cost which will allow to produce a significant number of direct dynamics trajectories. For a given initial condition, significant number of trajectories are required to make statistically meaningful predictions. The reaction energy profile of all the four halon molecules at PBE0/6-31G* level are shown in Figure 4.1. There is no zero point energy added for the given energies which are relative to the corresponding reactant energy. For better comparison of the dissociation energy profiles of halons molecules, the stationary point energies (in kcal/mol) at PBE0/6-31G* and CCSD(T)//MP2/aug-cc-pVTZ levels of theory are summarized in Table 4.5.

Table 4.5 : Comparison of stationary point energies (in kcal/mol) on the dissociation energy profiles of halons computed using PBE0/6-31G* and CCSD(T)//MP2/aug-cc-pVTZ level of theories. Energies given are relative to respective reactants and zero point energy corrected.

stationary point	PBE0/6-31G*	CCSD(T)
CF_2Cl_2	0.0	0.0
$Cl + CF_2Cl$	77.2	78.9
Iso-TS[a]	78.4	80.0
$F_2C-Cl-Cl$	69.1	69.3
$CF_2 + Cl_2$	80.8	71.3
TS1[b]	124.0	-
CF_2Br_2	0.0	0.0
$Br + CF_2Br$	64.0	69.4
Iso-TS[a]	67.7	73.1
$F_2C-Br-Br$	48.8	55.9
$CF_2 + Br_2$	57.3	58.9
TS1[b]	95.8	87.7
$CHBr_3$	0.0	0.0
$Br + CHBr_2$	58.3	65.9
Iso-TS[a]	59.1	61.4
$BrHC-Br-Br$	46.7	49.9
$CHBr + Br_2$	89.1	89.9
$CBr_2 + HBr$	63.9	65.9
CH_2BrCl	0.0	0.0
$Cl + CH_2Br$	76.1	79.1
$Br + CH_2Cl$	64.9	70.7
Iso-TS1A[c]	69.5	68.9
$CH_2-Cl-Br$	60.8	59.2
TS2[d]	104.1	97.1
$CHCl + HBr$	87.2	79.6
Iso-TS1B[e]	74.7	71.3
$CH_2-Br-Cl$	61.4	58.0
TS3[f]	110.7	101.8
$CHBr + HCl$	87.7	79.0

[a] connects reactant with the respective iso-halon species
[b] concerted TS connecting reactant with the $CF_2 + X_2$ products
[c] connects reactant with $CH_2-Cl-Br$ isomer
[d] connects reactant with the $CHCl + HBr$ products
[e] connects reactant with $CH_2-Br-Cl$ isomer
[f] connects reactant with the $CHBr + HCl$ products

Dissociation chemistry of Halons in the gas-phase were simulated using Born-Oppenheimer direct chemical dynamics simulations[Sun and Hase, 2003; Paranjothy *et al.*, 2013]. Classical trajectories were initiated from respective reactant wells using classical micro-canonical sampling technique[Hase and Buckowski, 1980; Peslherbe *et al.*, 1999]. A total energy of 150 kcal/mol was supplied to each halon molecule and it was distributed among all the normal modes of molecules. This amount of energy was selected so that all the possible dissociation pathways would be accessible. The gradients and potentials were computed on-the-fly from density functional PBE0/6-31G* electronic structure theory. The trajectories were integrated for a total time of 4 ps or until products have formed and reached a minimum separation of 12 Å. Integration step-size was kept at 0.5 fs with Velocity-Verlet integration[Swope *et al.*, 1982] scheme. This integration step-size was sufficient enough to make good energy conservation in the trajectories.

4.3 RESULTS AND DISCUSSION

4.3.1 Electronic Structure Calculations

As can be seen in Figure 4.1, the general characteristics of the energy profiles of CF_2Cl_2 and CF_2Br_2 molecules are similar. Reaction energy barrier for both the radical ($X + CF_2X$, X=Cl and Br) and the isomerization ($F_2C{-}X{-}X$) leading to molecular products $CF_2 + X_2$ pathways are competing in nature. For X=Cl (Br), 79.0 (65.3) and 79.5 (68.6) kcal/mol are the barriers for the radical and isomerization pathways, respectively. The iso-halon species containing halogen-halogen bond, for both the molecules, are weakly bound and present in shallow potential wells. For the molecular product channel, a symmetrical multi-center TS has been proposed earlier but was never found[Cameron and Bacskay, 2000; Kalume *et al.*, 2010].

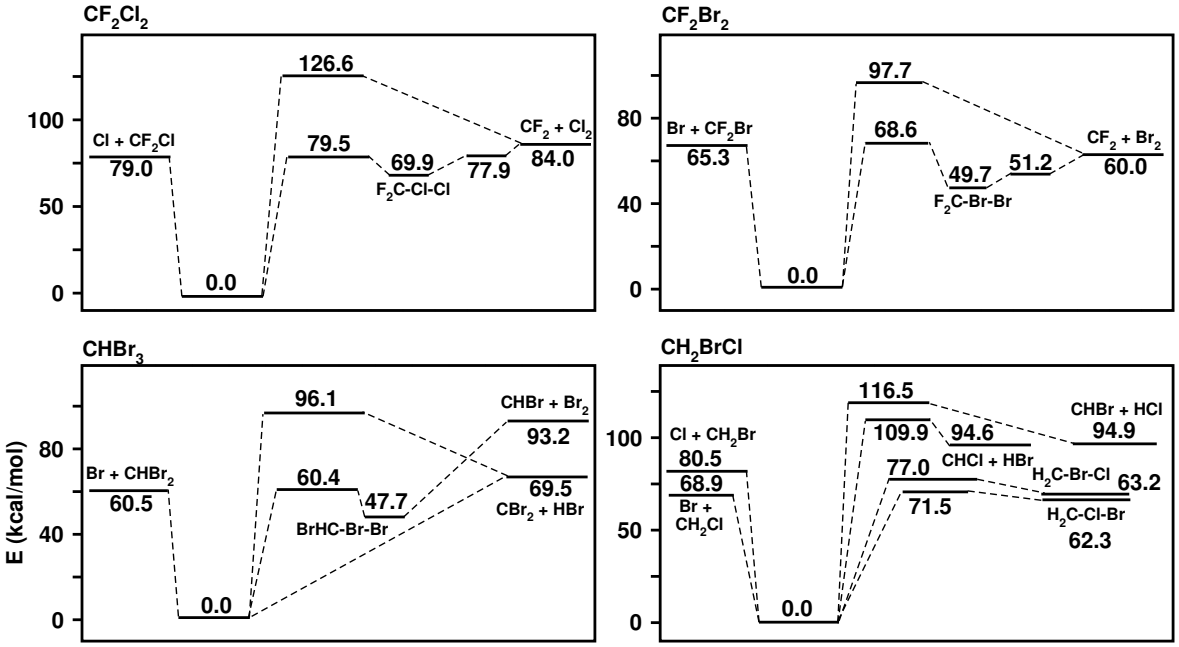

Figure 4.1 : Potential energy profiles of dissociation pathways of halons computed using density functional PBE0/6-31G* level of theory. Energies given are relative to that of respective reactants and are without zero point energy corrections.

In the present work, the multi-center TS for both the molecules were found and they exist at higher energy values with respect to the reactant molecules. Multi-center TS for CF_2Cl_2 molecule exists at 126.6 kcal/mol and for CF_2Br_2 at 97.7 kcal/mol and are consistent with previous predictions[Kalume *et al.*, 2010] about multi-center TSs. Intrinsic reaction coordinate (IRC) calculations were performed to confirm that these TSs connect the reactants with correct products. The results of IRC calculations are shown in Figure 4.2.

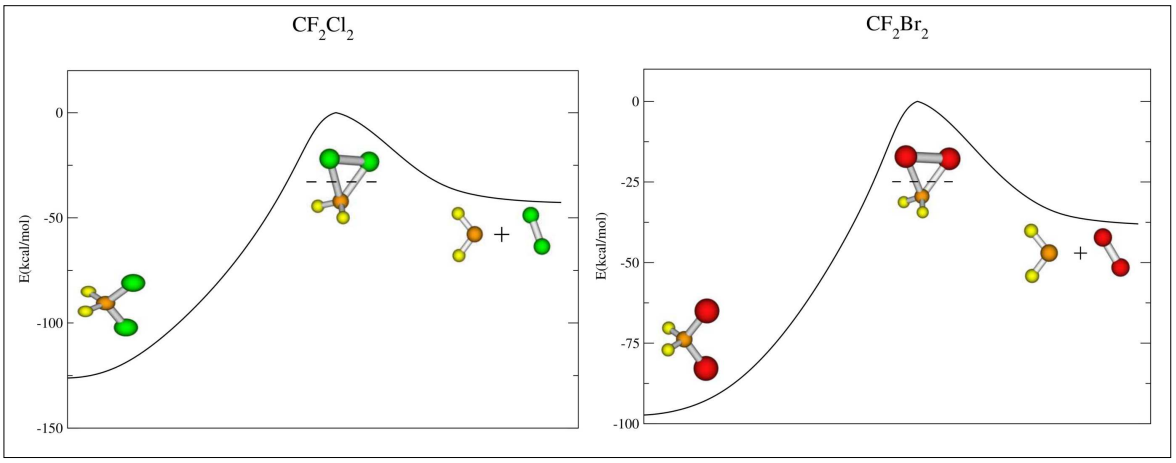

Figure 4.2 : Intrinsic reaction coordinate (IRC) data for the concerted elimination of X_2 from CF_2X_2 (X=Cl,Br) computed using PBE0/6-31G* theory. Energies are in units of kcal/mol.

There are two possible molecular product elimination pathways exist for $CHBr_3$ viz., Br_2 elimination and HBr elimination. The isomerization pathway leads to the molecular products CHBr + Br_2 (see Figure 4.1). The radical ($CHBr_2$ + Br) and molecular (CHBr + Br_2) pathways are iso-energetic in nature. Attempts to find the concerted transition state similar to CF_2X_2(X = Br, Cl) mentioned above were unsuccessful. CBr_2 + HBr elimination was also proposed in a previous work[Kalume *et al.*, 2010] via a high energy TS. Energy of the TS which connects the reactant to CBr_2 + HBr is 96.1 kcal/mol with respect to the reactant. This transition state lies at much higher energy (by ∼24 kcal/mol) compared to other molecular products CHBr + Br_2.

For the molecule CH_2BrCl, the radical Br and Cl eliminations have energy barrier of 68.9 and 80.5 kcal/mol, respectively. Two different isomeric forms viz., $H_2C{-}Br{-}Cl$ and $H_2C{-}Cl{-}Br$ are possible and lead to molecular products. These products lie at energy of 135.9 kcal/mol relative to the reactant molecule. The dehydrohalogenation pathway similar to $CHBr_3$ exists for CH_2BrCl molecule which leads to CHBr + HCl and CHCl + HBr as products. Reaction energy profile, characterizing all the possible dissociation pathways of CH_2BrCl are shown in Figure 4.1.

4.3.2 Direct Dynamics Simulations

A total of 800 classical trajectories (200 per molecule) at 150 kcal/mol energy value were generated in the simulations. The fraction of reactive trajectories within the given 4 ps integration time was 68.0, 99.0, 100.0, and 98.5% for CF_2Cl_2, CF_2Br_2, $CHBr_3$, and CH_2BrCl, respectively. Detailed analysis of the trajectories were done to understand the reaction mechanisms for all the four molecules.

4.3.3 CF_2Cl_2 and CF_2Br_2

For the molecules CF_2Cl_2 and CF_2Br_2, the number of trajectories that showed reaction within the specified integration time was 136 and 198, respectively. The characteristics of the potential energy surface of these two molecules are similar, and the dynamics are not expected to differ significantly. In the dynamics calculations, the observed decomposition mechanisms were similar for both the molecules. But, the number of trajectories following a particular pathway was different. Both radical ($X + CF_2X$) and molecular (CF_2 + X_2) products were observed for both the molecules. Radical products were observed in 23 (X=Cl) and 46 (X=Br) trajectories which are 17 and 23 % of total reactive fractions. Previous studies have shown that the molecular products

can be produced via a high energy multi-center TS[Cameron and Bacskay, 2000]. Kalume et al., have reported electronic structure calculations[Kalume *et al.*, 2010] exploring the molecular product formation via isomerization (F_2C-X-X) and subsequent dissociation. Along with these pathways, another radical recombination pathway leading to the same molecular products were observed in the simulations. In this pathway, the C−X dissociation happens primarily but the reaction products do not separate immediately. After a small time interval, the X radical abstracts the other X from CF_2X radical and results in molecular products. In few of these trajectories, X showed movement around CF_2X at larger distances indicating a possible *roaming* mechanism[Suits, 2008].

Table 4.6 : Summary of trajectory events of CF_2Cl_2 and CF_2Br_2 dissociation.

pathway	X=Cl	X=Br
$\mathbf{X + CF_2X}$	23	46
$\mathbf{CF_2 + X_2}$		
concerted	0	18
isomerization	89	93
radical recombination	23	31
$\mathbf{CFX + FX}$	1	10
unreactive	64	2

Out of the 200 trajectories for CF_2Cl_2 and CF_2Br_2 molecules, 112 and 142 trajectories resulted in molecular products, respectively. Summary of the trajectory results following above mentioned three pathways are shown in Table 4.6. Since the concerted TS for CF_2Cl_2 lies at 126.6 kcal/mol (see Figure 4.1), none of the trajectories followed this high energy route to form the molecular products. For CF_2Br_2, concerted TS lies at quite lower (97.7 kcal/mol) energy, so 18 trajectories followed this route. This suggests that higher energy concerted pathway might be preferred at high energies/temperatures. The molecular product formation via isomerization (F_2C-X-X) occurred in 89 and 93 trajectories for X=Cl and Br, respectively. Reactant molecule first isomerizes to F_2C-X-X followed by subsequent dissociation of C−X bond to form $CF_2 + X_2$. These iso-halon species lie in a shallow potential energy well, hence they might have short lifetimes. Calculated trajectory averaged lifetime of the iso-halon species were 62 and 24 fs for $F_2C-Cl-Cl$ and $F_2C-Br-Br$, respectively. Lifetime were computed as the time difference at which X−X formation and subsequent C−X bond dissociation occurred. Criteria for the X−X bond formation was used as the equilibrium distance (2.4 Å for X=Cl and 2.5 Å for Br) and for the C−X dissociation, 0.5 Å above the C−X equilibrium distances were used.

Figures 4.3 and 4.4 show snapshots of example trajectories dissociated via above mentioned dissociation channels along with corresponding bond distances for the CF_2Cl_2 and CF_2Br_2 molecules, respectively. Figure 4.3(a) shows the snapshots of a trajectory showing $CF_2Cl_2 \longrightarrow CF_2 + Cl_2$ reaction via isomerization pathway. The isomer formation and its subsequent dissociation can be seen in the 690 and 785 fs frame, respectively. Similarly, Figure 4.4(b) shows the trajectory snapshots of CF_2Br_2 molecule where isomerization happens at 545 fs with a lifetime of ∼60 fs before further dissociation. This isomer species ($F_2C-Br-Br$) has been detected in the photo-dissociation experiment of CF_2Br_2 in an Ar matrix[George *et al.*, 2010]. It is clear from Table 4.6 that isomerization plays a central role in the molecular product formation for both the molecules. Figure 4.4(a) shows snapshots of an example $CF_2Br_2 \longrightarrow CF_2 + Br_2$ trajectory dissociating via concerted pathway. This concerted elimination of Br_2 via multi-center TS can be seen in the 95 fs frame. In order to further distinguish between the concerted and

isomerization mechanisms observed in CF_2Br_2, the time gap distribution between the two C−Br bond dissociations was calculated and are shown in Figure 4.4(e). The time gap is the difference in time instances where each of the C−Br bond distance reach to a critical value of 3.5 Å. Different distributions were observed for both concerted and isomerization pathways. The highest time-gap observed for the concerted trajectories reached up to 50 fs whereas for isomerization trajectories, it extends up to 500 fs. Molecular products formation via the indirect radical recombination route were observed in 23 (X=Cl) and 31 (X=Br) trajectories. Figure 4.3(b) shows trajectory snapshots of CF_2Cl_2 molecule following the indirect radical recombination pathway. In this trajectory, first C−Cl bond dissociates and Cl atom moves away from central C atom as far as 7 Å before coming back for the abstraction of the second Cl atom. Figure 4.3(c) shows the C−Cl bond distances with time which clearly differentiates the isomerization and radical recombination (via roaming) mechanisms. In an infrared multi-photon disintegration study[Chowdhury, 1991] of CF_2Cl_2, fast and slow components of CF_2 elimination were observed. This might have been due to the two different mechanisms for CF_2 formation, mentioned above.

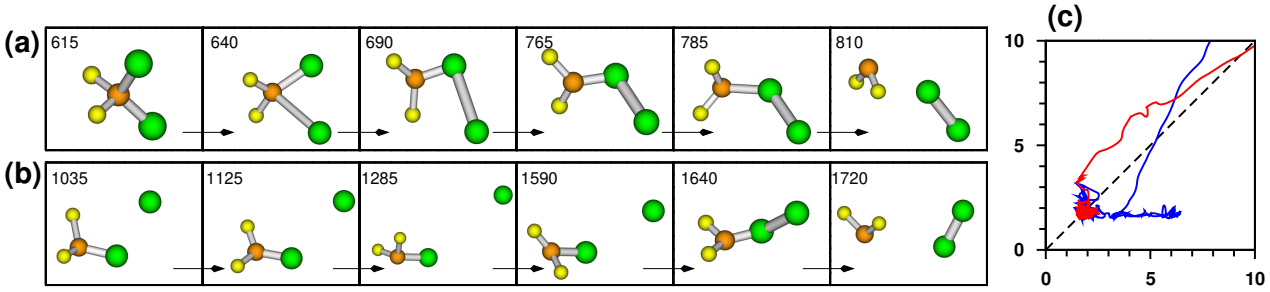

Figure 4.3 : Snapshots of $CF_2Cl_2 \longrightarrow CF_2 + Cl_2$ trajectories dissociating via (a) isomerization and (b) roaming pathway. (c) shows C−Cl(1) and C−Cl(2) bond distances (in Å) for the isomerization (red) and roaming (blue) trajectories. The numbers present inside each frame is time in fs.

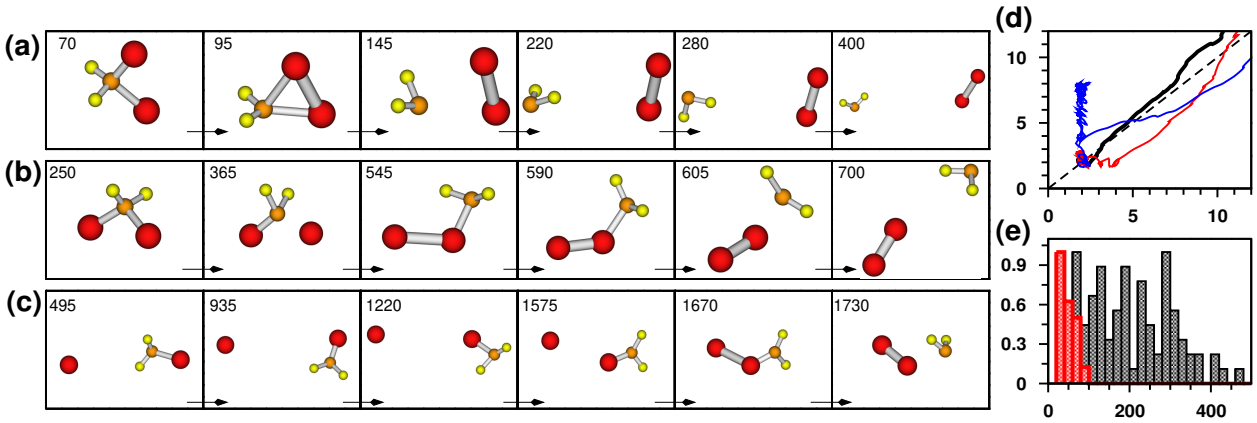

Figure 4.4 : Snapshots of $CF_2Br_2 \longrightarrow CF_2 + Br_2$ trajectories dissociating via (a) concerted (b) isomerization and (c) roaming pathway. Number inside each frame is time in fs at which the snapshot was taken. (d) shows C−Br(1) and C−Br(2) bond distances (in Å) for the concerted (black), isomerization (red), and roaming (blue) trajectories. Distributions of time gaps (in fs) between the two C−Br bond cleavages dissociating via isomerization (black) and the concerted (red) pathway are shown in (e).

In the present work, 15 out of 31 radical recombination trajectories of CF_2Br_2 followed roaming mechanism where Br atom moved away almost 8.0 Å from the central C atom. This process was predicted by George et al.,[George *et al.*, 2010] in their matrix isolation photolysis experiments on CF_2Br_2 and the present simulations confirm this prediction. Figure 4.4(c) shows the trajectory snapshots of a roaming trajectory, where C−Br bond dissociates and Br radical moves almost 8.0 Å before coming back for the abstraction of the other Br atom. This is a common mechanism observed for both the CF_2Cl_2 and CF_2Br_2 molecules and this indicates the general nature of this roaming mechanism for such molecules. Two C−Br bond distances (in Å) as a function of time are shown in Figure 4.4(d) for all the three types of trajectories discussed. The black, red, and blue colored lines represent concerted elimination, dissociation via isomerization, and radical recombination pathway, respectively. Time gap distributions (in fs) between the two C−Br bond distances dissociating via isomerization (black) and the concerted (red) pathway are shown in Figure 4.4(e) and this clearly shows higher time gap value for the isomerization pathway.

Wagner and co-workers[Kumaran *et al.*, 1995], in their shock-wave induced thermal decomposition study of CF_2Cl_2, observed subsequent dissociation of CF_2Cl. However, this subsequent reaction resulting in $CF_2X \longrightarrow CF_2 + X$ was not observed in the present work for both X=Cl and Br, probably due to energy constraints i.e. sufficient amount of energy was not available for further dissociation of CF_2X after the primary dissociation. Energy required for the secondary dissociation of CF_2Cl is ∼49 kcal/mol[Kumaran *et al.*, 1995]. The minor reaction products of CF_2Br_2 observed in the simulations are briefed discussed here. In 10 trajectories of CF_2Br_2, high energy products $CFBr + FBr$ were observed through isomerization involving Br−F bond. Energy of these products is 107.0 kcal/mol relative to the reactant. Out of the 10 trajectories, 6 dissociated via the isomer BrFC−F−Br, one via the isomer BrFC−Br−F and three via Br radical formation followed by F atom abstraction from CF_2Br. When there is more than one type of halogen atom, probability of migration of heavier atom is high. This trend has been observed in experiments[Lee and Bersohn, 1982; Maier *et al.*, 1990] and the present results are in agreement with this observation. For CF_2Cl_2, only one trajectory resulted in $CFCl + FCl$ products. It has to be noted here that 64 trajectories of CF_2Cl_2 did not dissociate during the entire 4 ps integration time. However, C−Cl bond dissociation occurred in many of these trajectories but they underwent further recombinations back to the reactant.

4.3.4 $CHBr_3$

All the 200 trajectories of $CHBr_3$ showed reaction during the 4 ps integration time. Radical products $CHBr_2 + Br$ were observed in 16 trajectories. Two types of molecular products are possible for $CHBr_3$ resulting in $Br_2 + CHBr$ and $HBr + CBr_2$. Energy is 23.7 kcal/mol higher for $Br_2 + CHBr$ products than the $HBr + CBr_2$ products. Consistently, the former channel was followed in 31 trajectories and the latter in 153 trajectories. Zou et al., have reported that the $CBr_2 + HBr$ products have the lowest enthalpy of reaction (59.0 kcal/mol) among all possible decomposition pathways[Zou *et al.*, 2004]. Out of the 31 trajectories that led to the elimination of Br_2, 19 dissociated via the isomer BrHC−Br−Br with a reaction barrier of 60.4 kcal/mol. Figure 4.5(a) shows snapshots of an example trajectory dissociating via this pathway and corresponding bond distances are shown in 4.5(c). The isomer formation can be seen in the 255 fs frame and it has a lifetime of ∼150 fs in this trajectory. The remaining 12 trajectories followed the radical recombination channel similar to that of CF_2Cl_2 and CF_2Br_2. The cleavage of C−Br bond led to radical products and then the second Br atom was abstracted from $CHBr_2$. Among these radical recombination trajectories, roaming by Br radical was observed in one trajectory.

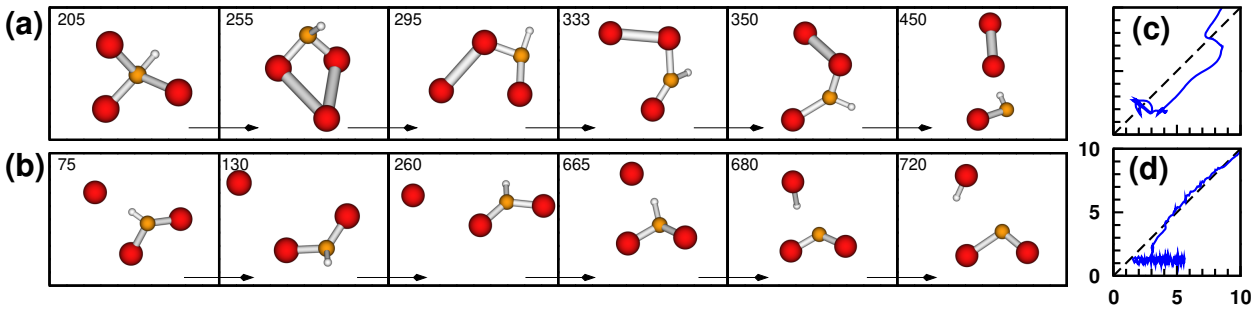

Figure 4.5 : Snapshots of a $CHBr_3$ trajectory forming (a) $Br_2 + CHBr$ and (b) $HBr + CBr_2$ products. (c) shows C−Br(1) and C−Br(2) distances for the trajectory given in (a). (d) shows C−Br distance in x-axis and C−H distance in y-axis for the trajectory shown in (b). The bond distances are given in units of Å.

The iso-form of $CHBr_3$ has been studied extensively. For instance, George et al.,[George *et al.*, 2011] have studied the structure and properties of this isomer. Two different pathways, recombination and direct pathway, leading to the formation of isomer have been experimentally[Carrier *et al.*, 2010] reported. Further, different time scales to distinguish these two pathways have been established in transient infrared absorption study of $CHBr_3$ photo-dissociation[Pal *et al.*, 2013; Preston *et al.*, 2013]. These observations along with present simulations show the importance of the iso-form in $CHBr_3$ decomposition. None of the trajectories showed concerted Br_2 elimination. Huang et al.,[Huang *et al.*, 2004] predicted the concerted elimination of Br_2 from photolysis of $CHBr_3$, eventhough, in a few experimental studies it has been reported that Br_2 is not the main product of $CHBr_3$ dissociation[McGivern *et al.*, 2000; Zou *et al.*, 2004]. In the present work, the Br_2 elimination pathway was not observed as a primary pathway (in comparison to CF_2Cl_2 and CF_2Br_2), which is consistent with these predictions. As mentioned above, two types of molecular products are possible for $CHBr_3$ and among them the dominant channel was dehydrohalogenation resulting in $CBr_2 + HBr$. The maximum number of trajectories (153 out of 200) followed this channel via two different mechanisms. One is concerted mechanism that occurs via a high energy multi-center TS which was identified in the present electronic structure theory calculations. The energy of this multi-center TS is 96.1 kcal/mol with respect to the reactant (see Figure 4.1), and this TS has not been reported previously. A total of 110 out of 153 trajectories followed concerted pathway to give the products. The other mechanism to form the $CBr_2 + HBr$ products is the radical recombination, and this was observed in 43 trajectories. In radical recombination mechanism, first C−Br bond dissociates followed by abstraction of H atom to give $CBr_2 + HBr$. In some of these trajectories, isomerization happened but then the trajectory showed recrossing to the reactant configuration. Roaming by Br radical around the $CHBr_2$ was observed in 11 trajectories. Figure 4.5(b) shows the snapshots of an example trajectory following the roaming mechanism to give $CBr_2 + HBr$ as final products. The C−Br and C−H bond distances corresponding to this trajectory are given in the x- and y-axis, respectively, of 4.5(d). The Br atom moved 6.0 Å away from the central C atom before coming back and abstracting the H atom. Note that water catalyzed conversion of $CHBr_3$ to HBr has been reported[Kwok *et al.*, 2004]. Reid and coworkers suggested that the dehydrogenation of haloalkanes might be of the proton-coupled electron transfer reaction[Kalume *et al.*, 2013]. The subsequent dissociation of the $CHBr_2$ was not observed in the simulations due to high energy barriers ($\sim$ 68.0 - 73.6 kcal/mol with respect to the energy of $CHBr_2$, computed at the MP2/6-311+G* theory[McGivern *et al.*, 2000]).

4.3.5 CH_2BrCl

The molecule CH_2BrCl differs from the other three molecules mentioned above because its iso-form will have bonding between two different halogen atoms. In the simulations, various reaction products with 98.5 % total reactivity were observed. In general, the molecular products were dominant than the radical products. As shown in the reaction energy profile of CH_2BrCl molecule in Figure 4.1, energy barriers for radical pathways to eliminate Cl and Br radicals are 80.5 and 68.9 kcal/mol, respectively. Only 12 trajectories out of 200, followed the radical pathways to form $Br + CH_2Cl$ and $Cl + CH_2Br$ products. Among these, 11 trajectories dissociated to $Br + CH_2Cl$, and only one gave $Cl + CH_2Br$ products. Two types of iso-halon species are possible for this molecule viz. $H_2C{-}Cl{-}Br$ and $H_2C{-}Br{-}Cl$ which have transition state energies of 71.5 and 77.0 kcal/mol, respectively. Only $H_2C{-}Br{-}Cl$ isomer was observed in three trajectories and the other was not observed in any of the trajectories. Isomerization process is not significant for this molecule compared to the other systems considered in this work. The $H_2C{-}Br{-}Cl$ isomer, only led to the formation of radical products $Cl + CH_2Br$ and did not dissociate into high energy (135.8 kcal/mol) molecular products $CH_2 + BrCl$. This is in contrast with same scenario of other molecules for which the isomerization leads to molecular products.

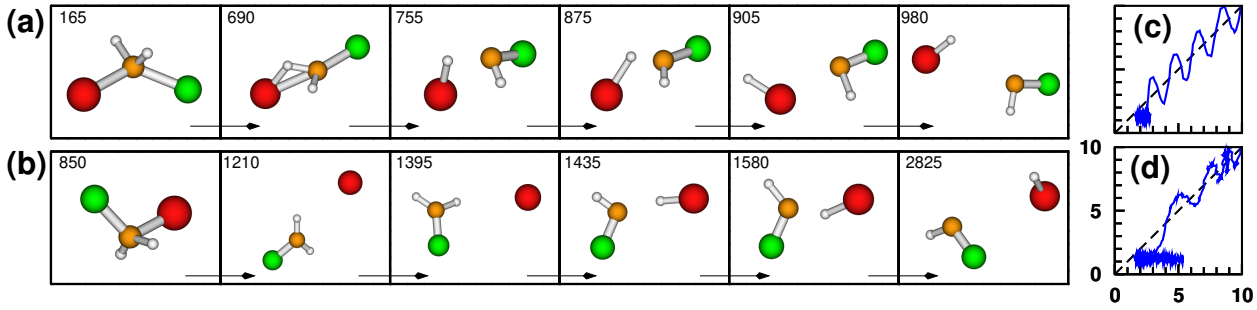

Figure 4.6 : Snapshots of CH_2BrCl trajectories forming $HBr + CHCl$ via (a) concerted and (b) radical recombination pathway. Corresponding time evolved $C{-}Br$ (x-axis) and $C{-}H$ (y-axis) distances (in Å) are given in (c) and (d).

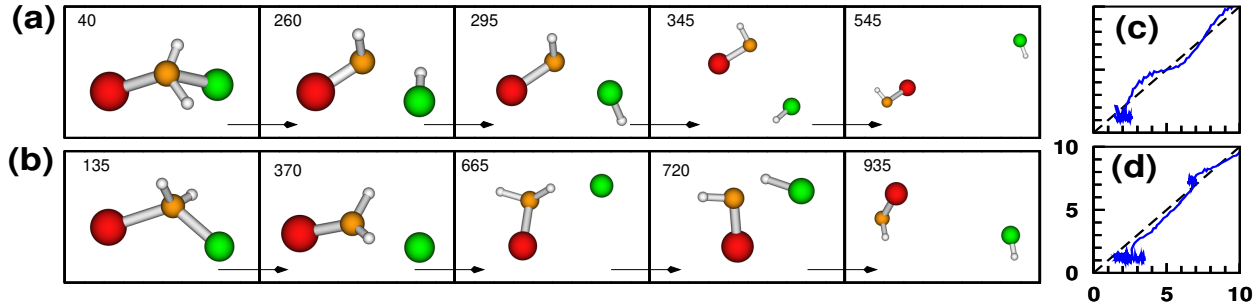

Figure 4.7 : Snapshots of trajectories showing $CH_2BrCl \longrightarrow HCl + CHBr$ reaction via (a) concerted and (b) radical recombinations. (c) and (d) show $C{-}Cl$ distance in x-axis and $C{-}H$ distance in y-axis in units of Å.

Two types of dehydrohalogenation products are possible for CH_2BrCl, resulting in $HBr + CHCl$ and $HCl + CHBr$ products. The energies of these products are almost same (see Figure 4.1). A total of 102, out of 200 trajectories resulted in the formation of $HBr + CHCl$ via two

different mechanisms. One is concerted via multi-center TS and the other is radical recombination method. Concerted pathway for $HBr + CHCl$ elimination has energy barrier of 109.9 kcal/mol above the reactant which were observed in 78 trajectories. In some of these trajectories, one of the isomer formed but recrossed back towards the reactant side. The other radical recombination pathway was observed in 24 trajectories. This occurred through the formation of Br radical followed by the abstraction of hydrogen atom from CH_2Cl. In Figure 4.6, snapshots of example trajectories giving $HBr + CHCl$ products via these two different mechanism are shown. In the recombination trajectory, Br radical moved 6.0 Å away before coming back to abstract the H atom.

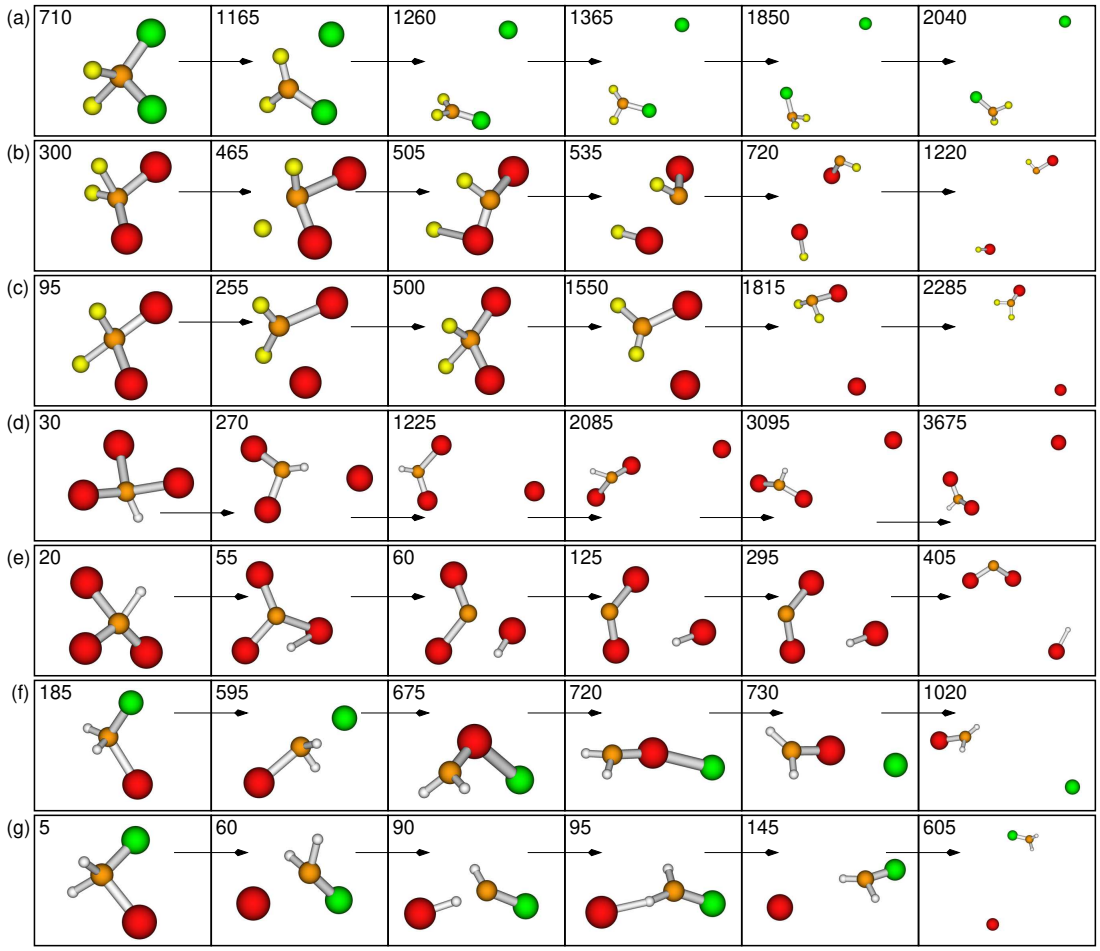

Figure 4.8 : Snapshots of trajectories showing (a) $CF_2Cl_2 \longrightarrow Cl + CF_2Cl$ radical dissociation (b) $CF_2Br_2 \longrightarrow CFBr + BrF$ reaction via isomerization (c) $CF_2Br_2 \longrightarrow Br + CF_2Br$ radical dissociation (d) $CHBr_3 \longrightarrow Br + CHBr_2$ radical dissociation (e) $CHBr_3 \longrightarrow HBr + CBr_2$ via concerted mechanism (f) $CH_2BrCl \longrightarrow Cl + CH_2Br$ via isomerization and (g) $CH_2BrCl \longrightarrow Br + CH_2Cl$ radical dissociation. Number inside each frame is time in fs at which the snapshot was taken.

The other molecular products $HCl + CHBr$ were observed in 80 trajectories. Similar to the earlier case, two different mechanisms were observed. The concerted pathway has energy barrier of 116.5 kcal/mol, which were observed in 69 trajectories and rest 11 trajectories followed radical pathway ($Cl + CH_2Br \longrightarrow HCl + CHBr$). Figure 4.7 shows snapshots of example trajectories forming both types of molecular products via two different mechanisms for elimination of

$Cl + CH_2Br \longrightarrow HCl + CHBr$. Figures 4.7(a) and (b) show concerted and radical recombination mechanisms, respectively. In the recombination trajectory, Cl radical moved 4.0 Å away before coming back to abstract the H atom. In the photolysis of bromomethane, CHBr and CHCl carbenes have been observed as an intermediate reaction[Yang *et al.*, 2010]. Snapshots of few more trajectories of all four molecules are shown in Figure 4.8. Figure 4.8(a) shows the snapshots of trajectory following the radical dissociation path $CF_2Cl_2 \longrightarrow Cl + CF_2Cl$. 4.8(b) shows the elimination of BrF via isomerization from $CF_2Br_2 \longrightarrow CFBr + BrF$, this was observed in 10 trajectories. 4.8(c), (d) shows Br radical dissociation from $CF_2Br_2 \longrightarrow Br + CF_2Br$ and $CHBr_3 \longrightarrow Br + CHBr_2$, respectively. Figure 4.8(e) shows the simultaneous removal of HBr from $CHBr_3$, HBr elimination via roaming mechanism was shown in Figure 4.5(b). In 4.8(f), (g) trajectory snapshots shows Cl and Br elimination from CH_2BrCl via isomerization and radical dissociation.

4.3.6 Discussion

The unimolecular decomposition of halon molecules has been the focus of various experimental and theoretical studies due to their widespread use in the past and their adverse effects on the environment. The dynamics simulations reported in this work show some general characteristics of halon decomposition. Trajectory results are summarized in Table 4.7 in the form of percentage of radical and molecular products for all the four molecules. The numbers shown in the table are the ratio of the number of trajectory forming a particular product and the total number of reactive trajectories multiplied by 100. Clearly, under current simulation conditions, the fraction of radical products formed is less than the molecular products for all the four molecules. However, several trajectories forming radical products followed the abstraction mechanisms (radical recombination) to form molecular products. A large fraction of trajectories followed radical recombinations route to give molecular products.

Table 4.7 : Fractions of radical and molecular products (in percentage) produced in the unimolecular decompositions of halons.

molecule	radical products	molecular products
CF_2Cl_2	**17.0** $Cl + CF_2Cl$ (17.0)	**83.0** $CF_2 + Cl_2$ (83.0)
CF_2Br_2	**23.0** $Br + CF_2Br$ (23.0)	**77.0** $CF_2 + Br_2$ (77.0)
$CHBr_3$	**8.0** $Br + CHBr_2$ (8.0)	**92.0** $CHBr + Br_2$ (15.5) $CBr_2 + HBr$ (76.5)
CH_2BrCl	**7.0** $Cl + CH_2Br$ (1.0) $Br + CH_2Cl$ (6.0)	**93.0** $HBr + CHCl$ (51.5) $HCl + CHBr$ (40.5) CH_2BrCl (1.0)

Different mechanisms were observed in the simulations indicating the rich chemistry of halons in the gas-phase. These mechanisms include concerted pathways via multi-center TSs, isomerization, and radical recombinations. The multi-center TSs were identified by electronic

structure calculations at high energy values compared to energies of other possible pathways. Concerted pathways via multi-center TSs were only observed when adequate amount of energy was available in the trajectories and may not be accessible in room temperature experiments. Based on dispersion fluorescence measurement and computational studies, Petro et al.,[Petro *et al.*, 2004] proposed the role of isomerization in decomposition of halons. The important role of isomerization in halon decomposition was discussed further by detailed characterization of the energy profile of the CF_2Cl_2, CF_2Br_2 and $CHBr_3$ dissociation.[Kalume *et al.*, 2010] The dynamics simulations reported in this work clearly shows the important role of isomerization in the dissociation of Halons. Isomerization pathways are iso-energetic to the C−X bond dissociations except for CH_2BrCl. A significant number of trajectories followed the iso-halons pathway for the CF_2Cl_2, CF_2Br_2, and $CHBr_3$ molecules. Further dissociation of radical products can also occur via isomerization. However, secondary dissociation were not observed probably due to energy constraints and limited integration time of trajectories. Radical recombination reactions observed in the simulations might account for the measurements reported by Huang et al.,[Huang *et al.*, 2004] and Xu et al.[Xu *et al.*, 2002] Excitation of $CHBr_3$ by near UV light results in fast C−Br bond cleavage[Peterson and Francisco, 2002] but the high quantum yield of Br_2 reported in these experiments might be due to the recombination reactions. Cartoni et al.,[Cartoni *et al.*, 2015] reported that radical products can form via isomerization pathway. They have reported that dissociation of diiodomethane radical cation into radical products (CH_2I++I) occurred via isomer ($[CH_2I_2]^{\cdot +} \longrightarrow [CH_2I{-}I]^{\cdot +} \longrightarrow CH_2I^+ + I$) species. However, radical product formation through isomerization was not seen in the simulations. The radical products were only observed by the C−X homolytic dissociation.

4.4 SUMMARY

The gas phase chemistry of four halon molecules (CF_2Cl_2, CF_2Br_2, $CHBr_3$, and CH_2BrCl) in the ground electronic state was studied by detailed electronic structure calculations and classical chemical dynamics simulations. Previous studies have shown that there are some unanswered questions about the decomposition mechanism of such molecules. One such issue is the role of iso-halons in dissociation, which had earlier been addressed using electronic structural theory calculations[Kalume *et al.*, 2010]. The dynamics studies reported here clearly demonstrates the importance of isomerization in the gas-phase chemistry of halons. An interesting aspect observed in the simulations was the radical recombination mechanism (to give molecular products) which involves roaming. Such mechanisms might be important in the gas phase experimental studies of halons[Krajnovich *et al.*, 1982; Kumaran *et al.*, 1995; Abel *et al.*, 1994]. Concerted mechanism also competes with radical recombination mechanism, although they have higher energy requirements. In summary, both radical recombination and concerted pathways depending upon experimental or simulation conditions leads to the formation of molecular products from halons. The initial conditions used in the present work correspond to thermal experiments rather than photochemical reactions. Internal conversion to ground state following photochemical excitations and subsequent ground state dissociation have been reported[Lin and Tsai, 2014; Huang *et al.*, 2004]. Cartoni et al. demonstrated that isomerization is not important for removing I_2 from $[CH_2I_2{}^{\cdot +}]$ cation in lower excitation electronic states[Cartoni *et al.*, 2015]. The explicit role of iso-halons in the excited state dissociation dynamics of halons has not been investigated. Only halomethanes were considered in the present work. The role of isomerization in the gas phase chemistry of polyalkylhalides, which are common in the natural environment, is another open area. Further detailed research is needed to address these issues.

…